0026-895X/04/6604-1061–1069$20.00
MOLECULAR PHARMACOLOGY
Copyright © 2004 The American Society for Pharmacology and Experimental Therapeutics
Mol Pharmacol 66:1061–1069, 2004

Vol. 66, No. 4
729/1178040
Printed in U.S.A.

Alkaloids Indolizidine 235B′, Quinolizidine 1-epi-207I, and the Tricyclic 205B are Potent and Selective Noncompetitive Inhibitors of Nicotinic Acetylcholine Receptors

Hiroshi Tsuneki, Yueren You, Naoki Toyooka, Syota Kagawa, Soushi Kobayashi, Toshiyasu Sasaoka, Hideo Nemoto, Ikuko Kimura, and John A. Dani

Department of Clinical Pharmacology (H.T., Y.Y., S.Ka., S.Ko., T.S., I.K.) and Faculty of Pharmaceutical Sciences (N.T., H.N.), Toyama Medical and Pharmaceutical University, Toyama, Japan, and Division of Neuroscience, Baylor College of Medicine, Houston, Texas (J.A.D.)

Received March 25, 2004; accepted July 6, 2004

ABSTRACT

Nicotinic acetylcholine receptors are key molecules in cholinergic transmission in the nervous system. Because of their structural complexity, only a limited number of subtype-specific agonists and antagonists are available to study nicotinic receptor functions. To overcome this limitation, we used voltage-clamp recordings to examine the effects of several frog skin alkaloids on acetylcholine-elicited currents in *Xenopus laevis* oocytes expressing major types of neuronal nicotinic receptors ($\alpha4\beta2$, $\alpha7$, $\alpha3\beta2$, $\alpha3\beta4$, and $\alpha4\beta4$). We found that the 5,8-disubstituted indolizidine (−)-**235B′** acted as a potent noncompetitive blocker of $\alpha4\beta2$ nicotinic receptors (IC_{50} = 74 nM). This effect was highly selective for $\alpha4\beta2$ receptors compared with $\alpha3\beta2$, $\alpha3\beta4$, and $\alpha4\beta4$ receptors. The inhibition of $\alpha4\beta2$ currents by (−)-**235B′** was more pronounced as the acetylcholine concentration increased (from 10 nM to 100 μM). Moreover, the blockade of $\alpha4\beta2$ currents by (−)-**235B′** was voltage-dependent (more pronounced at hyperpolarized potentials) and use-dependent, indicating that (−)-**235B′** behaves as an open-channel blocker of this receptor. Several other 5,8-disubstituted indolizidines (5-*n*-propyl-8-*n*-butylindolizidines), two 5,6,8-trisubstituted indolizidines ((−)-**223A** and (+)-6-epi-**223A**), and a 1,4-disubstituted quinolizidine ((+)-**207I**) were less potent than (−)-**235B′**, and none showed selectivity for $\alpha4\beta2$ receptors. The quinolizidine (−)-1-epi-**207I** and the tricyclic (+)-**205B** had 8.7- and 5.4-fold higher sensitivity, respectively, for inhibition of the $\alpha7$ nicotinic receptor than for inhibition of the $\alpha4\beta2$ receptor. These results show that frog alkaloids alter the function of nicotinic receptors in a subtype-selective manner, suggesting that an analysis of these alkaloids may aid in the development of selective drugs to alter nicotinic cholinergic functions.

Nicotinic acetylcholine receptors (nAChRs) are widely expressed in the mammalian brain, and act as key molecules in the physiological processes of reward, cognition, learning, and memory (Changeux et al., 1998; Dani, 2001; Lindstrom, 2003). Nicotinic receptors are ligand-gated ion channels composed of five subunits. To date, 12 nAChR subunits ($\alpha2$-$\alpha10$ and $\beta2$-$\beta4$ subunits) have been identified (Hogg et al., 2003). Because different combinations of these subunits produce different subtypes of receptors, the potential for nAChR diversity is vast. Based on their pharmacology, function, and location, different categories of nAChR subtypes have been created. Three predominant subtypes in the mammalian central nervous system are those containing the $\alpha7$ subunit ($\alpha7$*), the $\beta2$ subunit ($\beta2$*), or the $\beta4$ subunit ($\beta4$*) (Alkondon and Albuquerque, 1993; Zoli et al., 1998).

Evidence indicates that nAChRs are implicated in several neurological disorders. In particular, significant loss of $\alpha4\beta2$ nAChRs has been observed in cortical autopsies from patients with Alzheimer's disease, and schizophrenia and bipolar disorder exhibit some linkage to the $\alpha7$-subunit gene (Weiland et al., 2000). Mutations in the $\alpha4$ or the $\beta2$ subunit also underlie autosomal-dominant nocturnal frontal lobe epilepsy in some families (Raggenbass and Bertrand, 2002). Nicotinic agonists and antagonists would therefore be very

This work was supported in part by Smoking Research Foundation (Japan) (to I.K.) and by Grants-in-Aid 14771274 and 16590435 for Scientific Research from the Japanese Ministry of Science, Culture, Sports, and Technology (to H.T.). J.A.D. was supported by grants from the National Institute of Neurological Disorders and Stroke and National Institute on Drug Abuse of the National Institutes of Health (USA).
H.T. and Y.Y. contributed equally to this work.
Article, publication date, and citation information can be found at http://molpharm.aspetjournals.org.
doi:10.1124/mol.104.000729.

ABBREVIATIONS: BAPTA-AM, 1,2-*bis*(*o*-aminophenoxy)ethane-*N*,*N*,*N*′,*N*′-tetraacetic acid tetra(acetoxymethyl) ester; ACh, acetylcholine; DHβE, dihydro-β-erythroidine; MLA, methyllycaconitine; nAChR, nicotinic acetylcholine receptor.

valuable and are being investigated for possible use in these diseases (Lloyd and Williams, 2000; Dani et al., 2004). However, selective ligands for the multiple subtypes of neuronal nicotinic receptors are still scarce.

Extracts from the skin of certain poison frogs provide a variety of pharmacologically active alkaloids, and more than 500 alkaloids have been isolated to date (Daly et al., 1999). Some of them are known to target nAChRs: a nicotinic agonist, epibatidine, and nicotinic antagonists, histrionicotoxins, pumiliotoxins, and indolizidines (Spivak et al., 1982; Warnick et al., 1982; Aronstam et al., 1986; Daly et al., 1991, 1999). However, the selectivity of most amphibian alkaloids for each subtype of nAChR remains to be characterized. In the present study, we investigated the selectivity of bicyclic alkaloids, indolizidines, and quinolizidines, and a tricyclic alkaloid, 8*b*-azaacenaphthylene, across several major types of nicotinic receptors ($\alpha4\beta2$, $\alpha7$, $\alpha3\beta2$, $\alpha3\beta4$, and $\alpha4\beta4$) expressed in *Xenopus laevis* oocytes.

Materials and Methods

Materials. All alkaloids and their analogs used in this study were synthesized and are shown in Fig. 1. The synthesis of indolizidine (−)-**235B′** was performed as reported previously (Momose and Toyooka, 1994; Toyooka et al., 1997; Toyooka and Nemoto, 2002). The structure of (−)-**235B′** is identical to that of the natural product. The synthetic indolizidines (5-*n*-propyl-8-*n*-butylindolizidine) **I**, **II**, and **III** were synthesized, and indicated that **223I** was not a 5,8-disubstituted indolizdine. The synthesis of indolizidine **I** has been shown previously (Toyooka et al., 1997; Toyooka and Nemoto, 2002). The synthesis of 5,6,8-trisubstituted indolizidine (−)-**223A** along with revision of its structure has recently been reported (Toyooka and Nemoto, 2002; Toyooka et al., 2002) as well as the synthesis of a 6-epimer (**223A** proposed). This unnatural compound has been designated (+)-6-epi-**223A** in the present study. The 1,4-disubstituted quinolizidine (+)-**207I**, which is the opposite enantiomer of the natural product, was synthesized in recent studies (Toyooka and Nemoto, 2002, 2003). An unnatural 1-epimer of (+)-**207I**, named (−)-1-epi-**207I** in this study, was synthesized as described previously (Toyooka et al., 1997; Toyooka and Nemoto, 2002). Synthetic (+)-**205B** is the opposite enantiomer of natural (−)-**205B**, as reported by Toyooka et al. (2003).

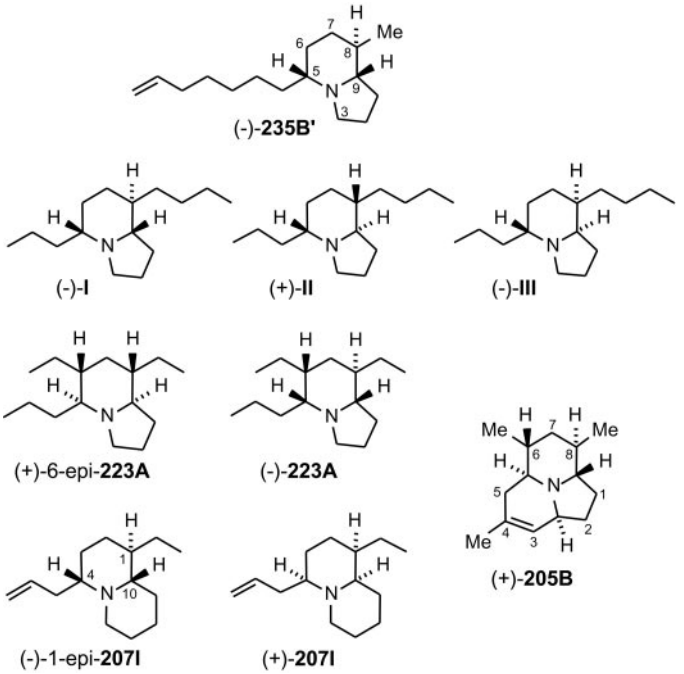

Fig. 1. Structures of frog skin alkaloids and their analogs. Absolute stereochemistry is as follows. (−)-**235B′**, 5*R*, 8*R*, 9*S*; (−)-**I**, 5*R*, 8*R*, 9*S*; (+)-**II**: 5*R*, 8*S*, 9*R*; (−)-**III**, 5*R*, 8*R*, 9*R*; (+)-6-epi-**223A**, 5*S*, 6*R*, 8*S*, 9*R*; (−)-**223A**, 5*R*, 6*R*, 8*R*, 9*S*; (−)-1-epi-**207I**, 1*R*, 4*S*, 10*S*; (+)-**207I**, 1*R*, 4*R*, 10*R*; (+)-**205B**, 2a*S*, 5a*S*, 6*R*, 8*R*, 8a*S*

The other reagents were purchased from Sigma (St. Louis, MO), unless indicated otherwise. BAPTA-AM was purchased from Calbiochem-Novabiochem Corp. (San Diego, CA).

The cDNAs of the rat $\alpha3$, $\beta2$, and $\beta4$ subunits in pcDNA1/Neo vectors were subcloned into HindIII and XhoI sites of pcDNA3.1 vectors (Invitrogen, Carlsbad, CA), and the cDNA of the rat $\alpha4$ subunit in pcDNA1/Neo vectors was subcloned into HindIII and XbaI sites of pcDNA3.1 vectors (Invitrogen) to enhance the expression of $\alpha3\beta2$, $\alpha3\beta4$, and $\alpha4\beta4$ nicotinic receptors in oocytes. To express $\alpha4\beta2$ and $\alpha7$ nAChRs, mouse cDNAs were used.

Expression in *X. laevis* Oocytes. All experiments were carried out in accordance with guidelines approved by the Toyama Medical and Pharmaceutical University Animal Research Committee. Oocytes were surgically removed from *X. laevis* frogs under anesthesia using Tricaine solution (2.4 g/l). The oocytes were rinsed in calcium-free OR2 buffer (82.5 mM NaCl, 2.5 mM KCl, 1 mM $MgCl_2$, and 5 mM HEPES, pH 7.6), then defolliculated in this buffer supplemented with 1.5 mg/ml collagenase A (Roche Diagnostics, Mannheim, Germany) for approximately 2 h at room temperature. Stage V-VI oocytes were selected and microinjected with 20 ng of cDNAs in the nucleus. The mixture of two subunit cDNAs, $\alpha3$ or $\alpha4$ in combination with $\beta2$ or $\beta4$, was injected in a ratio of 1:1, whereas $\alpha7$ subunit was injected alone. Oocytes were incubated at 19°C in standard oocyte saline solution (100 mM NaCl, 2 mM KCl, 1.8 mM $CaCl_2$, 1 mM $MgCl_2$, and 5 mM HEPES, 2.5 mM pyruvic acid, 1% BSA, and 25 μg/ml gentamycin, pH 7.5) for 3 to 8 days before recordings were made.

Electrophysiological Recording. An oocyte was placed in a 300-μl tube-like chamber in which Ringer's solution (82.5 mM NaCl, 2.5 mM KCl, 2.5 mM $CaCl_2$, 1 mM $MgCl_2$, and 5 mM HEPES, pH 7.4) containing 1 μM atropine to block endogenous muscarinic receptors was perfused by gravity (15 ml/min). Current responses were recorded under two-electrode voltage-clamp at a holding potential of −60 mV using a GeneClamp 500 amplifier and pClamp7 software (Axon Instruments, Union City, CA). The sampling rate was 20 Hz. Electrodes contained 3 M KCl and had resistances of <1 MΩ.

To apply a pulse of acetylcholine (ACh) to the oocyte, the perfusion fluid was switched to one containing ACh for 5 s, using a three-way Teflon solenoid valve (Parker Hannifin Corp., General Valve Division, Fairfield, NJ) controlled by a PC computer with pClamp7 software. A 3-min wash between ACh applications produced reproducible control currents with no obvious desensitization. For responses in alkaloids (test responses), the perfusion fluid was stopped during alkaloid application for 3 min to conserve the compounds. Perfusion was started again 0.5 min before measuring responses to ACh in the presence of test alkaloid.

Control experiments in the Ca^{2+} chelator BAPTA were performed to minimize the activation of endogenous Ca^{2+}-activated chloride channels in *X. laevis* oocytes. Those endogenous currents were prevented by BAPTA to be sure that they did not alter the pharmacological profiles of the tested alkaloids. Oocytes were loaded with BAPTA by incubating in a SOS solution containing BAPTA-AM (100 μM) for 4 h before recording, as described previously (Ibanez-Tallon et al., 2002). Otherwise, oocytes were incubated with a low-Ca^{2+} Ringer's solution (82.5 mM NaCl, 2.5 mM KCl, 0.5 mM $CaCl_2$, 2 mM $MgCl_2$, and 5 mM HEPES, pH 7.4) to depress the endogenous chloride conductance while we investigated the mechanism of receptor blockade by the alkaloids.

Data Analysis. The average peak amplitudes of three control responses to ACh (1 μM for $\alpha4\beta2$ and $\alpha4\beta4$ receptors; 100 μM for $\alpha7$, $\alpha3\beta2$, and $\alpha3\beta4$ receptors) just preceding exposure to alkaloids were

used to normalize the amplitude of each test response. These ACh concentrations were determined to be approximately 30% of the maximum effective concentrations (EC_{30}), according to the ACh-concentration response curve (data not shown). Each data point of the concentration-response curve represents the average value ± S.E.M. of measurements from at least three oocytes.

Concentration-inhibition curves for alkaloids (antagonists) were fitted by a nonlinear regression to the equation: $I = I_{max} - I_{max}/[1 + (IC_{50}/An)^{nH}]$, where I_{max} is the maximal normalized current response (in the absence of antagonist for inhibitory curves), An is the antagonist concentration, IC_{50} is the antagonist concentration eliciting half-maximal current, and n_H is the Hill coefficient. Curve fittings were analyzed using Prism software (GraphPad Software, Inc., San Diego, CA). For antagonist efficacy curves, I_{max} was constrained to 1 and I_{min} was constrained to 0.

The ACh concentration-response curves for $\alpha4\beta2$ nicotinic receptors were fitted to the following two-component (double sigmoid) equation using Prism software (GraphPad Software, Inc.): $y = y_{max} \times [a1/(1 + (EC_{50,high}/x)^{nH,high}) + (1 - a1)/(1 + (EC_{50,low}/x)^{nH,low})]$, where y is the percentage amplitude, a1 is the percentage of receptors in the high-affinity component, high and low refer to relative ACh sensitivity, x is the acetylcholine concentration, and n_H is the Hill coefficient. Responses evoked by 1 mM ACh corresponded to 100% activation of the high- and low-affinity components. y_{max} is the maximal current amplitude (percentage), normalized by the amplitude of ACh (1 mM)-evoked currents in the absence of alkaloid. Moreover, fits to a single-component (sigmoid) equation $y = y_{max} \times [1/(1 + (EC_{50}/x)^{nH}]$ were performed, and relative improvements between the single-component fit and the two-component fit were assessed by using GraphPad Prism to calculate the *F*-statistic from the ratios of the minimum sums of squares of deviations.

Statistical Analysis. The significance of differences between two groups was assessed by Student's *t* test, and the significance of differences between multiple groups were assessed by one-way analysis of variance followed by the Dunnet's multiple range test. Values of *P* less than 0.05 were considered significant.

Results

The subtype selectivity of the frog alkaloids was investigated across five recombinant nAChRs ($\alpha4\beta2$, $\alpha7$, $\alpha3\beta2$, $\alpha3\beta4$, and $\alpha4\beta4$) expressed in *X. laevis* oocytes. The oocytes were voltage-clamped, and application of 0.1 to 1000 μM ACh elicited inward currents. When the currents were elicited by the EC_{30} doses of ACh (see *Data Analysis*), $\alpha4\beta2$ and $\alpha3\beta2$ heteromeric receptors showed faster decay kinetics than $\beta4$-containing heteromeric receptors ($\alpha3\beta4$ and $\alpha4\beta4$), and currents through $\alpha7$ homomeric receptors decayed very rapidly during the ACh application (Fig. 2, A and B). These features were consistent with previous observations (Alkondon and Albuquerque, 1993; Chavez-Noriega et al., 1997; Fenster et al., 1997). We also confirmed that the ACh responses in oocytes expressing $\alpha4\beta2$ nAChRs were inhibited by 5 μM dihydro-β-erythroidine (DHβE, a competitive neuronal nAChR antagonist acting preferentially on non-$\alpha7$ receptor) and $\alpha7$ nAChRs were inhibited by 10 nM methyllycaconitine (MLA, an antagonist of $\alpha7$-containing nicotinic receptors) (Fig. 2A). The $\alpha4\beta2$ nAChR-mediated currents gradually recovered during a 25-min washout of DHβE, whereas $\alpha7$ nAChR-mediated currents were completely recovered 15 min after removal of MLA.

The responses mediated by recombinant nAChRs were blocked by most of the alkaloids used, as summarized in Table 1. When the oocytes expressing $\alpha4\beta2$ nAChR were treated with indolizidine (−)-**235B′** (0.3 μM), the peak amplitude of the ACh-elicited currents was greatly decreased (Fig. 2B). This blocking effect was reversible within 10 min (data not shown). Compared with the efficacy on oocytes expressing the other receptor subtypes, (−)-**235B′** blocked the $\alpha4\beta2$ receptor-mediated responses (IC_{50} = 74 nM, n_H = 0.47 ± 0.04) with 6.0-fold higher sensitivity than blockade of $\alpha7$ receptor-mediated responses (IC_{50} = 442 nM, n_H = 0.48 ± 0.05), 40.5-fold higher than that of $\alpha3\beta2$ receptor-mediated ones (IC_{50} = 3.0 μM, n_H = 0.74 ± 0.05), 51.4-fold higher than that of $\alpha3\beta4$ receptor-mediated ones (IC_{50} = 3.8 μM, n_H =

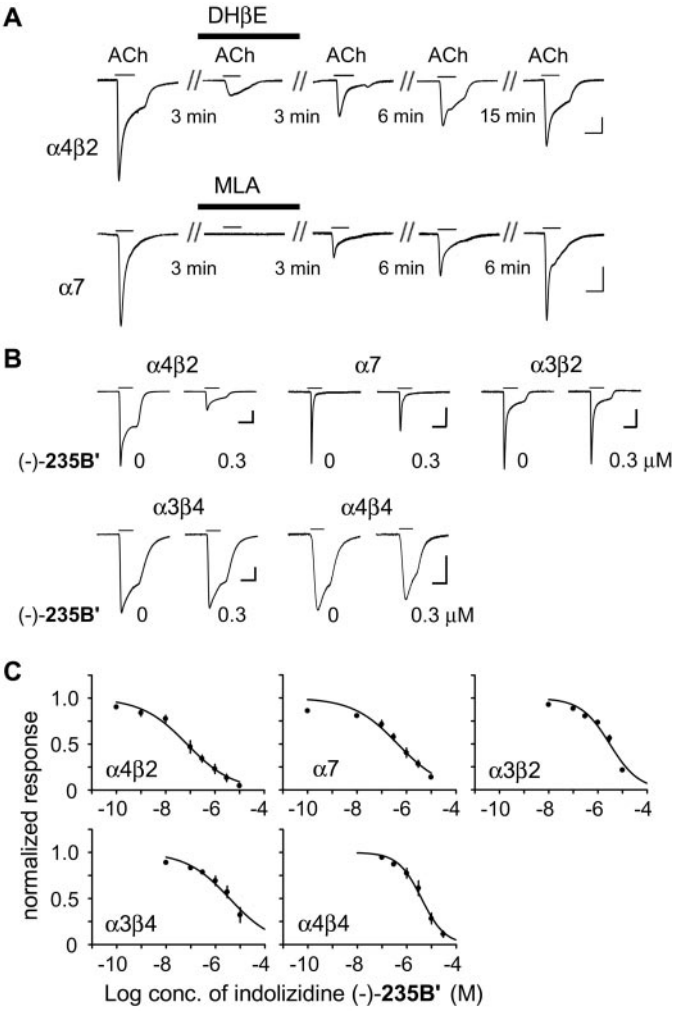

Fig. 2. Inhibitory effects of indolizidine (−)-**235B′** on ACh-induced currents in *X. laevis* oocytes expressing recombinant nicotinic receptors. Currents were recorded in voltage-clamp mode at −60 mV. A, typical traces showing inhibition by DHβE (5 μM) on $\alpha4\beta2$ currents elicited by ACh (1 μM) and inhibition by MLA (10 nM) on $\alpha7$ currents elicited by ACh (100 μM). Horizontal bars indicate the period of perfusion with ACh for 5 s. Vertical scale bars represent 1 μA for $\alpha4\beta2$ currents, and 0.5 μA for $\alpha7$ currents. The ACh-elicited currents recovered after removals of these antagonists. B, representative traces showing the ACh-elicited currents in the absence and presence of (−)-**235B′** (0.3 μM). Concentrations near the 30% effective doses (EC_{30}) of ACh were used to elicit the currents (*i.e.* 1 μM for $\alpha4\beta2$ and $\alpha4\beta4$ receptors and 100 μM for $\alpha7$, $\alpha3\beta2$, and $\alpha3\beta4$ receptors). For test responses, oocytes were preincubated with (−)-**235B′** for 3 min and then exposed to ACh with (−)-**235B′**. Horizontal bars, 5 s. Vertical scale bars represent 1 μA for $\alpha4\beta2$ currents, and 0.5 μA for $\alpha7$, $\alpha3\beta2$, $\alpha3\beta4$, and $\alpha4\beta4$ currents. C, concentration-response curves for (−)-**235B′** on recombinant nicotinic receptors. Current responses to ACh in the presence of (−)-**235B′** in each oocyte were normalized to the ACh responses (control responses) recorded in the same oocytes. Values represent the mean ± S.E.M. for five to nine separate experiments.

0.49 ± 0.07), and 54.1-fold higher than that of $\alpha4\beta4$ receptor-mediated ones (IC_{50} = 4.0 μM, n_H = 0.91 ± 0.10) (Fig. 2, B and C).

To exclude the possibility that indolizidine (−)-**235B′** blocks nAChR signaling downstream, such as endogenous Ca^{2+}-activated chloride channels that could amplify the nAChR responses in *X. laevis* oocytes, BAPTA control experiments were performed. Oocytes were incubated with the membrane-permeable Ca^{2+} chelator, BAPTA-AM, before recording. Similar blocking actions of indolizidine (−)-**235B′** were observed in the BAPTA-AM–treated oocytes expressing $\alpha4\beta2$ nAChRs. Compared with untreated oocytes, the peak amplitude of the currents elicited by ACh (1 μM) in the absence of (−)-**235B′** was 459 ± 46 nA (3 oocytes), and in the presence of 0.1 and 0.3 μM (−)-**235B′**, the amplitudes were decreased to 58.0 ± 3.2 and 35.7 ± 6.8%, respectively. These results indicate that indolizidine (−)-**235B′** directly blocks $\alpha4\beta2$ nAChRs.

Analysis of the $\alpha4\beta2$ peak current amplitude revealed that the ACh concentration-response curves were not adequately described by a single Hill equation (Fig. 3A, dashed line, EC_{50} = 10.9 μM and n_H = 0.52). A significantly better fit was obtained with the sum of two Hill equations (Fig. 3A, continuous line), indicating the existence of a high- and low-affinity component (Zwart and Vijverberg, 1998; Covernton and Connolly, 2000; Buisson and Bertrand, 2001; Nelson et al., 2003; Almeida et al., 2004; Khiroug et al., 2004). The high-affinity coefficients were $EC_{50,high}$ = 1.3 μM and $n_{H,high}$ = 0.56, whereas the low-affinity coefficients were $EC_{50,low}$ = 119 μM and $n_{H,low}$ = 1.5. The fractions of high- and low-affinity components were 58.3 and 41.7%, respectively. In the presence of indolizidine (−)-**235B′** (0.1 μM), the ACh concentration-response curve shifted downward, and the responses to ACh at the maximal concentration (1 mM) did not reach the levels observed in the absence of (−)-**235B′** (Fig. 3A). These results indicate that indolizidine (−)-**235B′** is not acting as a competitive antagonists of $\alpha4\beta2$ receptors. The concentration-response relationship for ACh in the presence of (−)-**235B′** was well fit by a single Hill equation (Fig. 3A, dashed line, EC_{50} = 8.8 μM and n_H = 0.44). When we applied the two-component model to the data, the fit obtained is shown as the continuous line in Fig. 3A, yielding the high-affinity coefficients of $EC_{50,high}$ = 0.07 μM and $n_{H,high}$ = 0.85 and the low-affinity coefficients of $EC_{50,low}$ = 24.8 μM and $n_{H,low}$ = 1.0. The fractions of high- and low-affinity components were 31.0 and 69.0%, respectively.

To know the mode of the receptor blockade by (−)-**235B′**, $\alpha4\beta2$ receptors were activated by increasing concentrations of ACh (ranging from 10 nM to 1 mM) in the presence of (−)-**235B′** (0.1 μM). The ACh-elicited currents were measured in a lower external Ca^{2+} concentration (0.5 mM) to avoid the Ca^{2+}-activated chloride conductance. As shown in Fig. 3B, the relative blockade by (−)-**235B′** was larger at the higher concentrations of ACh. Thus, in the presence of the alkaloid (−)-**235B′** at a constant concentration (0.1 μM), the peak amplitudes of currents elicited by ACh at 0.1 and 100 μM were reduced by 32.8 ± 5.8 and 71.5 ± 3.4%, respectively; differences were statistically significant ($P < 0.01$, determined by unpaired Student's t test).

Moreover, the voltage dependence of the blocking effects of (−)-**235B′** on $\alpha4\beta2$ currents was explored at different holding potentials (from −140 to +40 mV) in 20-mV steps. The currents were elicited by ACh (1 μM) in 0.5 mM Ca^{2+}. As shown in Fig. 4A, the current-voltage relationship showed strong inward rectification for the ACh (1 μM)-elicited current at positive membrane potentials. Exposure to (−)-**235B′** (0.1 μM) induced a reduction of the peak amplitude of currents, and the magnitude of this reduction was more pronounced at hyperpolarized potentials. (−)-**235B′** blocked the $\alpha4\beta2$ currents by 68 ± 6% at −140 mV and by only 38 ± 6% at −40 mV (Fig. 4B).

We also investigated whether (−)-**235B′** produces a use-dependent blockade of $\alpha4\beta2$ receptors. When oocytes expressing $\alpha4\beta2$ receptors were stimulated with short pulses of ACh (10 μM, 200 ms) every 8 s in 0.5 mM Ca^{2+}, consistent, repeatable currents were obtained. Figure 5A shows a typical

TABLE 1
Potency of blocking effects of frog skin alkaloids on *X. laevis* oocytes expressing recombinant nicotinic receptors

	IC_{50} (95% CI)			n
	$\alpha4\beta2$ (1 μM ACh)	$\alpha7$ (100 μM ACh)	$\alpha3\beta4$ (100 μM ACh)	
		μM		
(−)-**235B′**	0.07 (0.05, 0.11)	0.4 (0.3, 0.6)	3.8 (2.3, 6.1)	5–8
(−)-**I**[a]	6.0 (4.1, 8.8)	3.4 (1.7, 6.7)	>10.0	3–5
(+)-**II**	16.8 (13.2, 21.3)	2.5 (1.8, 3.5)	14.7 (11.1, 19.5)	3–5
(−)-**III**	20.1 (11.7, 34.3)	1.8 (1.6, 2.1)	3.0 (2.2, 4.0)	3–7
(+)-6-epi-**223A**	>30.0	>30.0	15.1 (10.3, 22.3)	3–5
(−)-**223A**	4.5 (3.7, 5.5)	4.2 (3.6, 4.8)	14.1 (9.9, 20.2)	5–7
(−)-1-epi-**207I**	5.2 (4.2, 6.5)	0.6 (0.4, 0.9)	8.8 (4.7, 16.6)	3–5
(+)-**207I**	5.0 (2.5, 9.8)	3.4 (2.5, 4.6)	N.D.	3
(+)-**205B**	13.5 (9.0, 20.2)	2.5 (1.6, 4.1)	11.3 (6.5, 19.8)	4–6

95% CI, 95% confidence intervals; N.D., not determined; n, number of data
[a] This compound will be designated as natural **223W**.

recording in one oocyte. In contrast, when (−)-**235B′** (0.1 μM) was superfused in the bath for 15 s preceding ACh application, then the responses to the repetitive pulses of ACh co-applied with (−)-**235B′** (0.1 μM) were progressively decreased in the same oocyte (Fig. 5A). Figure 5B summarizes the results obtained during the first 64 s in different oocytes. We further studied whether the blocking effect of (−)-**235B′** (0.1 μM) depends on the frequency of the ACh pulses. Using a lower frequency (16-s interval) rather than 8-s interval of stimulation, we found a significant difference in the extent of the blockade of α4β2 currents at the two frequencies (Fig. 5B). At any time point tested, (−)-**235B′** produced a stronger blockade of the currents elicited by ACh pulses at the higher frequency (8-s interval) than at the lower frequency (16-s interval).

Next, we tested the effects of another type of the 5,8-disubstituted indolizidine analogs, 5-*n*-propyl-8-*n*-butylindolizidines **I**, **II**, and **III**, on the ACh-elicited currents in oocytes expressing recombinant nicotinic receptors. These three compounds are stereoisomers, and **I** has the same stereochemistry as (−)-**235B′** at the 5 and 9 positions (5,9-*cis*: 5,9*Z*), as shown in Fig. 1. The alkaloid **I** at 10 μM blocked the responses mediated by α4β2 receptors and α7 receptors similarly (Fig. 6A). In fact, these currents were blocked by this alkaloid in a concentration-dependent manner, with IC_{50} values of 6.0 μM for α4β2 currents and 3.4 μM for α7 currents (Fig. 6B, Table 1). In contrast, the indolizidines **II** and **III** were more potent at blocking the responses mediated by α7 receptors than α4β2 receptors (Table 1). In addition, the indolizidine **I** had a negligible effect on the α3β4 receptor responses at a high concentration (10 μM), whereas the responses through this receptor were substantially blocked by the indolizidine **II** (IC_{50} = 14.7 μM) and were potently blocked by the indolizidine **III** (IC_{50} = 3.0 μM).

Stereoselective pharmacological properties were also observed with the 5,6,8-trisubstituted indolizidines (+)-6-epi-**223A** and (−)-**223A**. The alkaloid (+)-6-epi-**223A** (10 μM) had a negligible effect on the ACh-elicited currents in oocytes expressing α4β2 or α7 receptors (Table 1), whereas (−)-**223A** (10 μM) blocked both the α4β2 and α7 receptor-mediated currents to a similar extent (Fig. 7A). (−)-**223A** blocked those

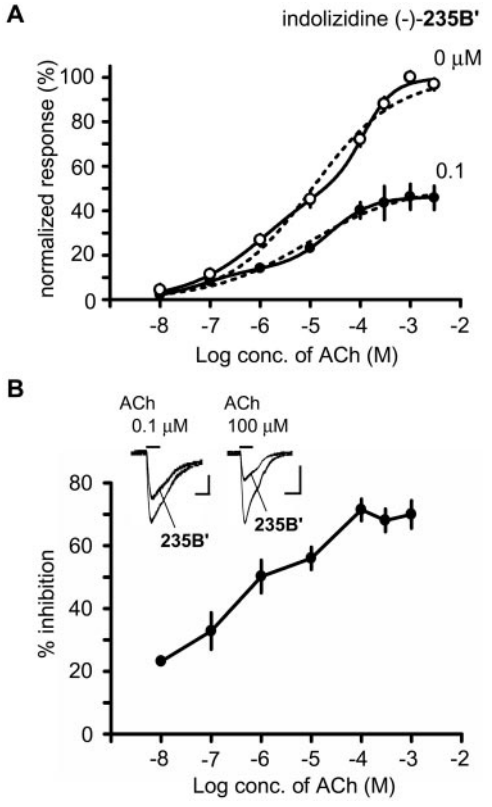

Fig. 3. Blockade by indolizidine (−)-**235B′** of the ACh-induced currents in oocytes expressing α4β2-nicotinic receptors is noncompetitive in nature. Currents were recorded in voltage-clamp mode at −60 mV. A, concentration response curves for ACh in the absence and presence of indolizidine (−)-**235B′**. Oocytes were preincubated with (−)-**235B′** (0.1 μM) for 10 min and then exposed to ACh (0.1 μM–1 mM) in the presence of (−)-**235B′** in standard Ringer's solution. Each current response to ACh in the presence of (−)-**235B′** was normalized to the maximal current evoked by 1 mM ACh alone recorded in the same oocyte. Values represent the mean ± S.E.M. for five to eight separate experiments. The dashed lines indicate the fits by a single Hill equation, whereas the continuous lines indicate the fits by the sum of two Hill equations. B, the percentage inhibition by (−)-**235B′** (0.1 μM) of the α4β2 currents that were elicited by different concentrations of ACh (ranging from 10 nM to 1 mM) in a lower external Ca^{2+} concentration (0.5 mM). Values represent the mean ± S.E.M. for five to eight separate experiments. Inset shows α4β2 currents elicited by two different concentrations of ACh (0.1 and 100 μM) in the absence and presence of (−)-**235B′** (0.1 μM). Horizontal bars, 5 s. Vertical scale bars represent 150 nA for the ACh (0.1 μM)-elicited currents and 1000 nA for the ACh (100 μM)-elicited currents.

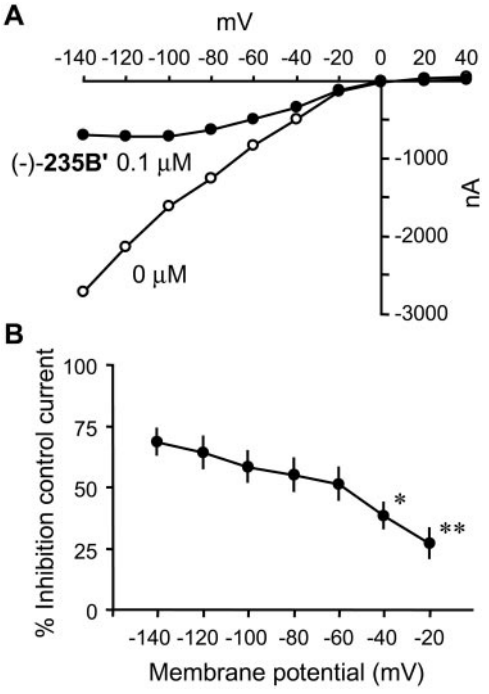

Fig. 4. Voltage-dependent effect of (−)-**235B′** on ACh-induced currents in oocytes expressing α4β2-nicotinic receptors. Oocytes were voltage-clamped at various membrane potentials (from −140 to +40 mV) in 20-mV steps. The currents were elicited by ACh (1 μM, 5 s), 3 min apart, at different holding potentials. This protocol was repeated in the same oocyte but in the presence of (−)-**235B′** (0.1 μM). (−)-**235B′** was present 3 min before application of ACh and throughout the latter experiments, including the ACh pulse. A, a typical plot demonstrating the current-voltage relationship in one oocyte expressing α4β2 receptors in the absence and presence of (−)-**235B′** (0.1 μM). B, averaged values for the inhibition by (−)-**235B′** of the ACh-elicited currents through α4β2 receptors. Data were expressed as percentage of inhibition of the control current obtained without (−)-**235B′** at each potential; the control current was considered the peak amplitude of ACh-induced current before the addition of (−)-**235B′**. Values represent the mean ± S.E.M. for six to nine separate experiments. *, $P < 0.05$; **, $P < 0.01$, compared with the (−)-**235B′**-induced inhibition of α4β2 currents at −140 mV.

two receptors in a concentration-dependent manner with IC_{50} values of about 4 μM (Fig. 7B, Table 1). The $\alpha3\beta4$ receptor-mediated currents were also blocked by (−)-**223A** with an IC_{50} value of 14 μM (Fig. 7, Table 1). This blocking effect was similar to that of (+)-6-epi-**223A** (IC_{50} = 15 μM).

The 1,4-disubstituted quinolizidine (−)-1-epi-**207I** selectively blocked $\alpha7$ receptor responses (IC_{50} = 0.6 μM), and it did so with 8.7-fold higher sensitivity than blockade of $\alpha4\beta2$ receptor responses (IC_{50} = 5.2 μM) and 14.7-fold higher than that of $\alpha3\beta4$ receptor responses (IC_{50} = 8.8 μM) (Table 1). The alkaloid (+)-**207I** equally blocked the responses mediated by $\alpha4\beta2$ receptors (IC_{50} = 5.0 μM) and $\alpha7$ receptors (IC_{50} = 3.4 μM).

When the oocytes expressing $\alpha7$ nAChRs were treated with 3 μM 8*b*-azaacenaphthylene (+)-**205B**, which is the unnatural enantiomer, the peak amplitude of the ACh-elicited currents was greatly decreased, whereas the responses via $\alpha4\beta2$ and $\alpha3\beta4$ nAChRs were not strongly affected (Fig. 8A). The blocking effect of (+)-**205B** (3 μM) on $\alpha7$ nAChRs was reversible within 10 min (data not shown). When the concentration-response curves were compared across these nAChR subtypes, (+)-**205B** blocked the $\alpha7$ receptor-mediated currents (IC_{50} = 2.5 μM, n_H = 0.46 ± 0.08) with 5.4-fold higher sensitivity than blockade of the $\alpha4\beta2$ receptor-mediated currents (IC_{50} = 13.5 μM, n_H = 0.44 ± 0.05) and 4.5-fold higher than blockade of the $\alpha3\beta4$ receptor-mediated currents (IC_{50} = 11.3 μM, n_H = 0.65 ± 0.13) (Fig. 8B, Table 1). These results indicate that (+)-**205B** selectively blocked the responses mediated by $\alpha7$ receptors, rather than $\alpha4\beta2$ and $\alpha3\beta4$ receptors. In the BAPTA-AM–treated oocytes expressing $\alpha7$ nAChRs, the peak amplitudes of the ACh (100 μM)-elicited currents were decreased by (+)-**205B** at 3 and 10 μM to 45.7 ± 6.3% and 11.7 ± 0.3% (three oocytes), respectively. These results demonstrate that (+)-**205B** directly blocks $\alpha7$ nAChRs.

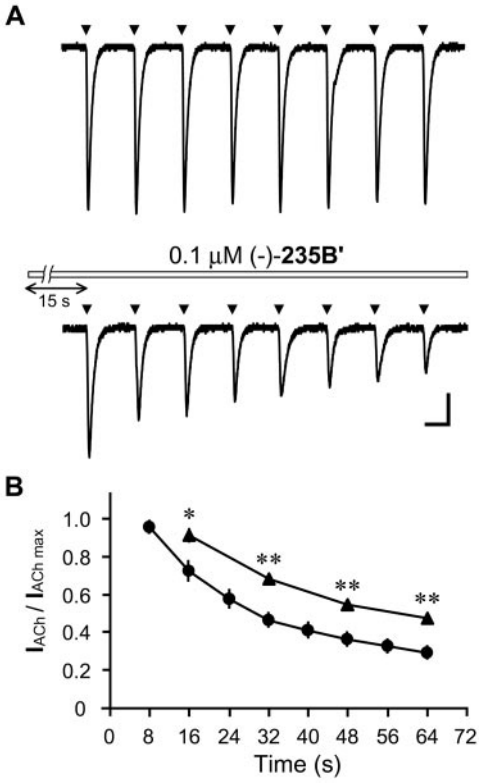

Fig. 5. Use-dependent blockade of $\alpha4\beta2$ currents by (−)-**235B′**. Oocytes expressing $\alpha4\beta2$ receptors were voltage-clamped at −60 mV, and the currents elicited every 8 or 16 s by short pulses of ACh (10 μM, 200 ms) were recorded in a lower external Ca^{2+} concentration (0.5 mM) until the currents became stable ($I_{ACh\ max}$). Thereafter, (−)-**235B′** (0.1 μM) was superfused in the bath for 15 s before ACh application, then the responses to the repetitive pulses of ACh coapplied with (−)-**235B′** (0.1 μM) were recorded in the same oocyte. A, top, a typical trace showing the stable currents elicited every 8 s by the ACh pulses (arrowheads) in the absence of (−)-**235B′**. Bottom, a typical trace showing the progressive inhibition of the ACh-elicited currents by (−)-**235B′**. Vertical scale bar, 100 nA; horizontal scale bar, 4 s. B, the ratios of the ACh-elicited currents in the presence of (−)-**235B′** (I_{ACh}) versus control $I_{ACh\ max}$ at two different frequencies. Values represent the mean ± S.E.M. in 10 and 7 separate oocytes at a higher (8-s interval) and a lower (16-s interval) frequency of ACh stimulation, respectively. *, $P < 0.05$; **, $P < 0.01$, compared with the ratios of $I_{ACh}/I_{ACh\ max}$ at the higher frequency (8 s) of ACh stimulation.

Discussion

The bicyclic "izidine" alkaloids (indolizidines, quinolizidines, pyrrolizidines, and azabicyclo[5.3.0]decanes) from amphibian skin have been examined. The alkaloids are mainly from neotropical dendrobatid frogs, *Dendrobates* spp., and most of the bicyclic alkaloids are known to be disubstituted, such as 5,8- or 3,5-disubstituted indolizidines and 1,4-disubstituted quinolizidines (Daly et al., 1999). Previously, it has been shown that particular 5,8-disubsutituted indolizidines, including (−)-**235B′**, act as noncompetitive nicotinic antagonists and inhibit carbamylcholine-elicited $^{22}Na^+$-influx via nAChR channels in PC-12 cells (Daly et al., 1991). In this study, we examined the selectivity of indoliz-

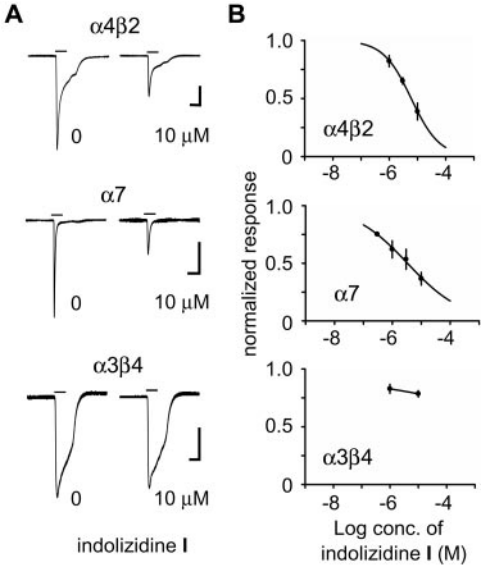

Fig. 6. Inhibitory effects of indolizidine **I** on ACh-induced currents in *X. laevis* oocytes expressing recombinant nicotinic receptors. Currents were recorded in voltage-clamp mode at −60 mV. A, representative traces showing the ACh-elicited currents in the absence and presence of the indolizidine **I** (10 μM). Horizontal bars indicate the period of perfusion with ACh for 5 s. Concentrations of ACh used were 1 μM for $\alpha4\beta2$ receptors and 100 μM for $\alpha7$ and $\alpha3\beta4$ receptors. For test responses, oocytes were preincubated with the indolizidine **I** for 3 min and then exposed to ACh with the indolizidine **I**. Vertical scale bars represent 1 μA for $\alpha4\beta2$ currents and 0.5 μA for $\alpha7$ and $\alpha3\beta4$ currents. B, concentration-response curves for the indolizidine **I** on recombinant nicotinic receptors. Current responses to ACh in the presence of the indolizidine **I** in each oocyte were normalized to the ACh responses (control responses) recorded in the same oocytes. Values represent the mean ± S.E.M. for three to five separate experiments.

idines for multiple subtypes of recombinant nAChRs expressed in oocytes. In addition, we examined the effects of several synthetic compounds with structures of frog alkaloids. Among these compounds, we found that indolizidine (−)-**235B′** was a highly potent blocker of $\alpha4\beta2$ nAChRs (IC_{50} = 0.07 μM). (−)-**235B′** seems to block via direct interaction with $\alpha4\beta2$ receptors, not through an indirect effect on the oocytes' endogenous Ca^{2+}-activated chloride channels.

The concentration-response relationship for ACh on $\alpha4\beta2$ nAChRs was best fit by the sum of two Hill equations. This finding is consistent with previous reports, indicating that there are at least two different populations of $\alpha4\beta2$ nAChRs with different affinities for ACh when ectopically expressed in *X. laevis* oocytes (Zwart and Vijverberg, 1998; Covernton and Connolly, 2000; Khiroug et al., 2004) and in HEK293 cell lines (Buisson and Bertrand, 2001; Nelson et al., 2003; Almeida et al., 2004). It has been proposed that these different properties are attributable to different subunit stoichiometries: the high-affinity nAChR is thought to be $(\alpha4)_2(\beta2)_3$, whereas the low-affinity nAChR is $(\alpha4)_3(\beta2)_2$ (Nelson et al., 2003).

The blockade of $\alpha4\beta2$ currents by (−)-**235B′** was more pronounced as the ACh concentrations increased (from 10 nM to 100 μM). If the low-affinity population of $\alpha4\beta2$ receptors were predominant compared with the high-affinity population in the present condition, selective blockade of the low-affinity receptors might explain the stronger effect of (−)-**235B′** on the responses to higher concentrations of ACh. In fact, the populations were almost equal between the high-affinity component (58.3%) and the low-affinity component (41.7%) based on the analysis of the ACh concentration-response curve (Fig. 3A). Furthermore, we estimate that activation of the high- and low-affinity receptors contributed to 58% and 42%, respectively, of the peak currents elicited by 1 μM ACh. The alkaloid (−)-**235B′** (0.1 nM-10 μM) blocked the ACh-elicited (1 μM) currents, and the concentration-response relationship for (−)-**235B′** was well described by a single sigmoid curve (Fig. 2C), without requiring a double sigmoid, indicating that (−)-**235B′** did not significantly differentiate between the high- and low-affinity receptors. Thus, the mode of action of (−)-**235B′** seems to be independent of these receptor populations. Because the probability of the $\alpha4\beta2$ nAChR-channel opening increases as the ACh concentration increases, (−)-**235B′** blocks the receptor-channels that are more frequently open at higher ACh concentrations by entering and occluding the open-channel pores. In general, open channel blockers are known to exhibit both a voltage-dependent and a use-dependent inhibition of nAChRs (Buisson and Bertrand, 1998; Pintado et al., 2000). Consistent with that expectation, we observed that (−)-**235B′** exerted stronger inhibition of the $\alpha4\beta2$ currents at hyperpolarized potentials. In addition, the $\alpha4\beta2$ currents elicited by repetitive ACh pulses were progressively inhibited by (−)-**235B′** in a use-dependent manner. Therefore, the mode of action of (−)-**235B′** is likely to be open channel blockade.

The sensitivity of indolizidine (−)-**235B′** for $\alpha4\beta2$ receptors was comparable with that of the best characterized antago-

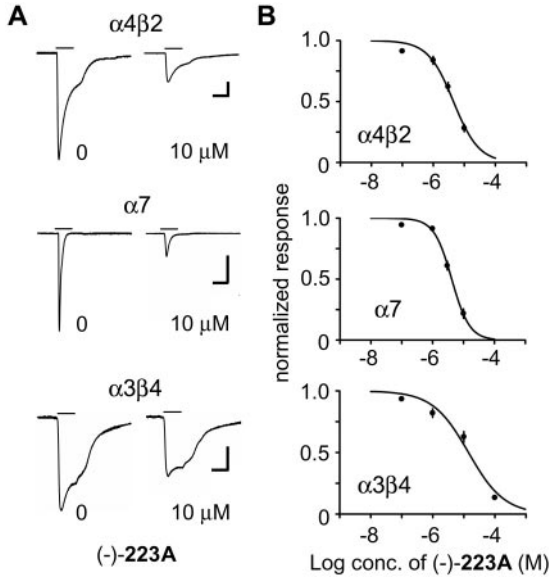

Fig. 7. Inhibitory effects of indolizidine (−)-**223A** on ACh-induced currents in *X. laevis* oocytes expressing recombinant nicotinic receptors. Currents were recorded in voltage-clamp mode at −60 mV. A, typical traces showing the ACh-elicited currents in the absence and presence of (−)-**223A** (10 μM). Horizontal bars indicate the period of perfusion with ACh for 5 s. Concentrations of ACh used were 1 μM for $\alpha4\beta2$ receptors and 100 μM for $\alpha7$ and $\alpha3\beta4$ receptors. For test responses, oocytes were preincubated with (−)-**223A** for 3 min and then exposed to ACh with (−)-**223A**. Vertical scale bars represent 1 μA for $\alpha4\beta2$ currents, and 0.5 μA for $\alpha7$ and $\alpha3\beta4$ currents. B, concentration-response curves for (−)-**223A** on recombinant nicotinic receptors. Current responses to ACh in the presence of (−)-**223A** in each oocyte were normalized to the ACh responses (control responses) recorded in the same oocytes. Values represent the mean ± S.E.M. for five to seven separate experiments.

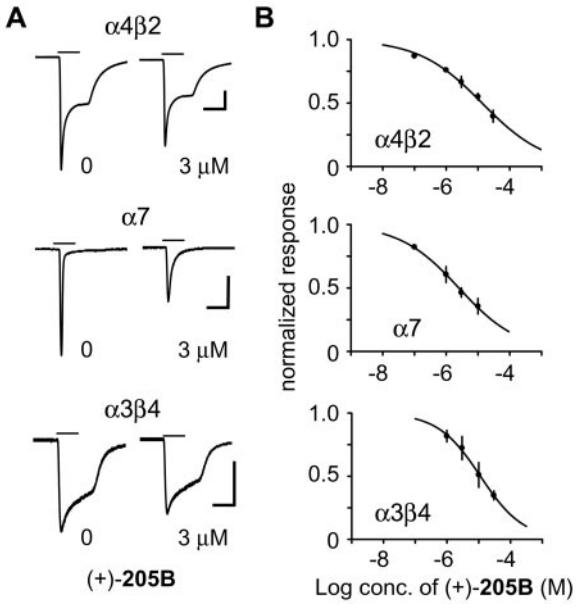

Fig. 8. Inhibitory effects of 8*b*-azaacenaphthylene (+)-**205B** on ACh-induced currents in *X. laevis* oocytes expressing recombinant nicotinic receptors. Currents were recorded in the voltage-clamp mode at −60 mV. Concentrations of ACh used were 1 μM for $\alpha4\beta2$ receptors and 100 μM for $\alpha7$ and $\alpha3\beta4$ receptors. For test responses, oocytes were preincubated with (+)-**205B** for 3 min and then exposed to ACh with (+)-**205B**. A, representative traces showing the ACh-elicited currents in the absence and presence of (+)-**205B** (3 μM). Horizontal bars indicate the period of perfusion with ACh for 5 s. Vertical scale bars represent 1 μA on $\alpha4\beta2$ receptor and 0.5 μA on $\alpha7$ and $\alpha3\beta4$ receptors. B, concentration-response curves for (+)-**205B** on recombinant nicotinic receptors. Current responses to ACh in the presence of (+)-**205B** in each oocyte were normalized to the ACh responses (control responses) recorded in the same oocytes. Values represent the mean ± S.E.M. for four to six separate experiments.

nist of $\alpha4\beta2$ nAChRs, DHβE, observed in *X. laevis* oocytes expressing human $\alpha4\beta2$ receptors (IC_{50} = 0.11 μM) (Chavez-Noriega et al., 1997). Moreover, (−)-**235B′** selectively blocked $\alpha4\beta2$ receptors more effectively than $\alpha3\beta2$ receptors (40.5-fold) or $\alpha3\beta4$ receptors (51.4-fold). These pharmacological properties are also comparable with DHβE. However, the selectivity for $\alpha4\beta2$ receptors over $\alpha7$ or $\alpha4\beta4$ receptors was different between (−)-**235B′** and DHβE: the rank order of potency of (−)-**235B′** was $\alpha4\beta2>\alpha7>\alpha3\beta2>\alpha3\beta4\approx\alpha4\beta4$, whereas that of DH$\beta$E is $\alpha4\beta4>\alpha4\beta2>\alpha3\beta2>\alpha3\beta4\approx\alpha7$ (Chavez-Noriega et al., 1997). It may be possible to develop even more potent and selective ligands on the basis of the structure of indolizidine (−)-**235B′**.

The structure of natural 5,6,8-trisubstituted indolizidine (−)-**223A** has recently been revised from (+)-6-epi-**223A** (Toyooka et al., 2002). It is interesting that (−)-**223A** but not (+)-6-epi-**223A** exhibited blocking effects on $\alpha4\beta2$ and $\alpha7$ receptors. These results suggest that the alkaloid (−)-**223A** may bind to the nAChRs in a stereoselective manner.

We also examined the stereoselective pharmacological properties of three stereoisomers, 5,8-disubstituted indolizidines **I**, **II**, and **III**. The indolizidine **I** has a 5,9-*cis* (5,9*Z*) structure, whereas the other two compounds have 5,9-*trans* (5,9*E*) structures. Because the indolizidine **I** exhibited a greater sensitivity to $\alpha4\beta2$ receptors than the indolizidines **II** and **III**, the 5,9-*cis* (5,9*Z*) structure may be important for binding to $\alpha4\beta2$ receptors with high affinity. Indeed, indolizidine (−)-**235B′** that possesses the 5,9-*cis* (5,9*Z*) structure was a potent blocker of $\alpha4\beta2$ receptors, as mentioned above. To test this hypothesis, it would be necessary to examine the effect of the (−)-**235B′** stereoisomer with a 5,9-*trans* (5,9*E*) structure on $\alpha4\beta2$ receptors in a future study.

The alkaloid (+)-**205B** has a unique tricyclic structure of 8*b*-azaacenaphthylene (Daly et al., 1999). No other alkaloids from amphibian skin are known to belong to this class. The absolute stereochemistry of this alkaloid was determined by the total synthesis (Toyooka et al., 2003). The alkaloid (+)-**205B** produced a selective inhibition of $\alpha7$ receptors over $\alpha4\beta2$ or $\alpha3\beta4$ receptors. We also found the high selectivity (8.7-fold) of 1,4-disubstituted quinolizidine (−)-1-epi-**207I** for $\alpha7$ receptors over $\alpha4\beta2$ receptors, which is greater than the $\alpha7$ selectivity (5.4-fold) of (+)-**205B**. Therefore, we suggest that a novel class of nicotinic antagonists may be developed based on the structure of these compounds.

In conclusion, we found that indolizidine (−)-**235B′** is a potent noncompetitive blocker of $\alpha4\beta2$ nAChRs, and its specificity is comparable with that of the competitive antagonist DHβE. We also found that quinolizidine (−)-1-epi-**207I** and tricyclic (+)-**205B** are selective blockers of $\alpha7$ nAChRs. It should also be noted that some of the alkaloids used in this study exhibited subtype-selective blockade of nAChRs in a stereoselective manner. These results suggest that it may be possible to obtain novel, potent, and subtype-selective blockers of nicotinic receptors by synthesizing stereoisomers of natural alkaloids. Thus, it is anticipated that the approach based on the frog alkaloids can provide lead compounds for the future design of drugs to treat cholinergic disorders in the central nervous system.

Acknowledgments

We are grateful to Dr. Jerry A. Stitzel (University of Colorado) and Dr. Jim Patrick (Baylor College of Medicine) for providing us with plasmid DNA. We would also like to thank Dr. Hideki Sakai (Toyama Medical and Pharmaceutical University) for the continuous support on data acquisition.

References

Alkondon M and Albuquerque EX (1993) Diversity of nicotinic acetylcholine receptors in rat hippocampal neurons. I. Pharmacological and functional evidence for distinct structural subtypes. *J Pharmacol Exp Ther* **265:**1455–1473.

Almeida LE, Pereira EF, Camara AL, Maelicke A, and Albuquerque EX (2004) Sensitivity of neuronal nicotinic acetylcholine receptors to the opiate antagonists naltrexone and naloxone: receptor blockade and up-regulation. *Bioorg Med Chem Lett* **14:**1879–1887.

Aronstam RS, Daly JW, Spande TF, Narayanan TK, and Albuquerque EX (1986) Interaction of gephyrotoxin and indolizidine alkaloids with the nicotinic acetylcholine receptor-ion channel complex of *Torpedo electroplax*. *Neurochem Res* **11:** 1227–1240.

Buisson B and Bertrand D (1998) Open-channel blockers at the human $\alpha4\beta2$ neuronal nicotinic acetylcholine receptor. *Mol Pharmacol* **53:**555–563.

Buisson B and Bertrand D (2001) Chronic exposure to nicotine upregulates the human $\alpha4\beta2$ nicotinic acetylcholine receptor function. *J Neurosci* **21:**1819–1829.

Changeux JP, Bertrand D, Corringer PJ, Dehaene S, Edelstein S, Léna C, Le Novere N, Marubio L, Picciotto M, and Zoli M (1998) Brain nicotinic receptors: structure and regulation, role in learning and reinforcement. *Brain Res Brain Res Rev* **26:**198–216.

Chavez-Noriega LE, Crona JH, Washburn MS, Urrutia A, Elliott KJ, and Johnson EC (1997) Pharmacological characterization of recombinant human neuronal nicotinic acetylcholine receptors h$\alpha2\beta2$, h$\alpha2\beta4$, h$\alpha3\beta2$, h$\alpha3\beta4$, h$\alpha4\beta2$, h$\alpha4\beta4$ and h$\alpha7$ expressed in *Xenopus* oocytes. *J Pharmacol Exp Ther* **280:**346–356.

Covernton PJ and Connolly JG (2000) Multiple components in the agonist concentration-response relationships of neuronal nicotinic acetylcholine receptors. *J Neurosci Methods* **96:**63–70.

Daly JW, Garraffo HM, and Spande TF (1999) Alkaloids from amphibian skins, in *Alkaloids: Chem and Biological Perspectives*, (Pelletier SW ed), vol. 13, pp 1–161, Pergamon Press, New York.

Daly JW, Nishizawa Y, Padgett WL, Tokuyama T, Smith AL, Holmes AB, Kibayashi C, and Aronstam RS (1991) 5,8-Disubstituted indolizidines: a new class of noncompetitive blockers for nicotinic receptor-channels. *Neurochem Res* **16:**1213–1218.

Dani JA (2001) Overview of nicotinic receptors and their roles in the central nervous system. *Biol Psychiatry* **49:**166–174.

Dani JA, De Biasi M, Liang Y, Peterson J, Zhang L, Zhang T, and Zhou F-M (2004) Potential applications of nicotinic ligands in the laboratory and clinic. *Bioorg Med Chem Lett* **14:**1837–1839.

Fenster CP, Rains MF, Noerager B, Quick MW, and Lester RA (1997) Influence of subunit composition on desensitization of neuronal acetylcholine receptors at low concentrations of nicotine. *J Neurosci* **17:**5747–5759.

Hogg RC, Raggenbass M, and Bertrand D (2003) Nicotinic acetylcholine receptors: from structure to brain function. *Rev Physiol Biochem Pharmacol* **147:**1–46.

Ibanez-Tallon I, Miwa JM, Wang HL, Adams NC, Crabtree GW, Sine SM, and Heintz N (2002) Novel modulation of neuronal nicotinic acetylcholine receptors by association with the endogenous prototoxin lynx1. *Neuron* **33:**893–903.

Khiroug SS, Khiroug L, and Yakel JL (2004) Rat nicotinic acetylcholine receptor $\alpha2\beta2$ channels: comparison of functional properties with $\alpha4\beta2$ channels in *Xenopus* oocytes. *Neuroscience* **124:**817–822.

Lindstrom JM (2003) Nicotinic acetylcholine receptors of muscles and nerves: comparison of their structures, functional roles and vulnerability to pathology. *Ann NY Acad Sci* **998:**41–52.

Lloyd GK and Williams M (2000) Neuronal nicotinic acetylcholine receptors as novel drug targets. *J Pharmacol Exp Ther* **292:**461–467.

Momose T and Toyooka N (1994) Asymmetric synthesis of the indolizidine alkaloids 207A, 209B and 235B′: 6-substituted 2,3-didehydropiperidine-2-carboxylate as a versatile chiral building block. *J Org Chem* **59:**943–945.

Nelson ME, Kuryatov A, Choi CH, Zhou Y, and Lindstrom J (2003) Alternate stoichiometries of $\alpha4\beta2$ nicotinic acetylcholine receptors. *Mol Pharmacol* **63:**332–341.

Pintado AJ, Herrero CJ, Garcia AG, and Montiel C (2000) The novel Na^+/Ca^{2+} exchange inhibitor KB-R7943 also blocks native and expressed neuronal nicotinic receptors. *Br J Pharmacol* **130:**1893–1902.

Raggenbass M and Bertrand D (2002) Nicotinic receptors in circuit excitability and epilepsy. *J Neurobiol* **53:**580–589.

Spivak CE, Maleque MA, Oliveira AC, Masukawa LM, Tokuyama T, Daly JW, and Albuquerque EX (1982) Actions of the histrionicotoxins at the ion channel of the nicotinic acetylcholine receptor and at the voltage-sensitive ion channels of muscle membranes. *Mol Pharmacol* **21:**351–361.

Toyooka N, Fukutome A, Nemoto H, Daly JW, Spande TF, Garraffo HM, and Kaneko T (2002) Synthesis of alkaloid 223A and a structural revision. *Org Lett* **4:**1715–1717.

Toyooka N, Fukutome A, Shinoda H, and Nemoto H (2003) Total synthesis of the antipode of alkaloid 205B. *Angew Chem Int Ed* **42:**3808–3810.

Toyooka N and Nemoto H (2002) Synthetic studies on dart-poison frog alkaloids. *Recent Res Dev Organic Chem* **6:**611–624.

Toyooka N and Nemoto H (2003) First enantioselective synthesis of (+)-quinolizidine 207I: determination of the absolute stereochemistry. *Tetrahedron Lett* **44:**569–570.

Toyooka N, Tanaka K, Momose T, Daly JW, and Garraffo HM (1997) High stereoselective construction of *trans*(2,3)-*cis*(2,6)-trisubstituted piperidines: an application to the chiral synthesis of *Dendrobates* alkaloids. *Tetrahedron* **53:**9553–9574.

Warnick JE, Jessup PJ, Overman LE, Eldefrawi ME, Nimit Y, Daly JW, and

Albuquerque EX (1982) Pumiliotoxin-C and synthetic analogues. A new class of nicotinic antagonists. *Mol Pharmacol* **22:**565–573.
Weiland S, Bertrand D, and Leonard S (2000) Neuronal nicotinic acetylcholine receptors: from the gene to the disease. *Behav Brain Res* **113:**43–56.
Zoli M, Léna C, Picciotto MR, and Changeux JP (1998) Identification of four classes of brain nicotinic receptors using β2 mutant mice. *J Neurosci* **18:**4461–4472.
Zwart R and Vijverberg HP (1998) Four pharmacologically distinct subtypes of α4β2 nicotinic acetylcholine receptor expressed in *Xenopus laevis* oocytes. *Mol Pharmacol* **54:**1124–1131.

Address correspondence to: Hiroshi Tsuneki, Department of Clinical Pharmacology, Toyama Medical and Pharmaceutical University, 2630 Sugitani, Toyama 930-0194, Japan. E-mail: htsuneki@ms.toyama-mpu.ac.jp